Chapter 6: Viscous Flow in Ducts

6.2 Stability and Transition

Stability: can a physical state withstand a disturbance and still return to its original state.

In fluid mechanics, there are two problems of particular interest: change in flow conditions resulting in (1) transition from one to another laminar flow; and (2) transition from laminar to turbulent flow.

(1) Transition from one to another laminar flow

(a) Thermal instability: Bernard Problem

A layer of fluid heated from below is top heavy, but only undergoes convective "cellular" motion for

Raleigh #: $Ra = \dfrac{g\alpha\Gamma d}{\upsilon w/d^2} = \dfrac{g\alpha\Gamma d^4}{k\nu} > Ra_{cr}$ $\qquad \dfrac{bouyancy\ force}{viscous\ force}$

α = *coefficient of thermal expansion* $= -\dfrac{1}{\rho}\left(\dfrac{\partial \rho}{\partial T}\right)_P$

$\Gamma = \Delta T / d = -{}^{dT}\!/_{dz}$ $\quad \rho = \rho_0\left(1 - \alpha \Delta T\right)$

d = depth of layer

k, ν =thermal, viscous diffusivities

w=velocity scale: convection ($w\Gamma$) = diffusion ($k\Gamma/d$) from energy equation, i.e., $w=k/d$

Solution for two rigid plates:

$Ra_{cr} = 1708$ *for progressive wave disturbance*

$\alpha_{cr}/d = 3.12$ $w = \hat{w} e^{i\alpha(x-ct)} = e^{c_i t}[\cos(x-ct) + \sin(x-ct)]$

$\lambda_{cr} = 2\pi/\alpha = 2d$ $T = \hat{T} e^{i\alpha(x-ct)}$

$\alpha = \alpha_r$ $c = c_r + ic_i$ For temporal stability

$\alpha_r = 2\pi/\lambda$ = *wavenumber*

c_r = *wave speed*

c_i : > 0 *unstable*
$= 0$ *neutral*
< 0 *stable*

Ra > 5 x 10^4 transition to turbulent flow

Thumb curve: stable for low Ra < 1708 and very long or short λ.

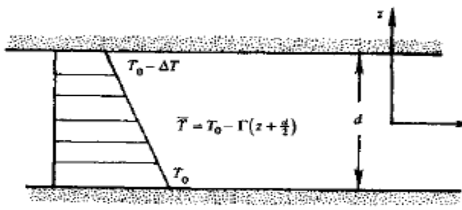

Fig. 11.2 Definition sketch for the Bénard problem.

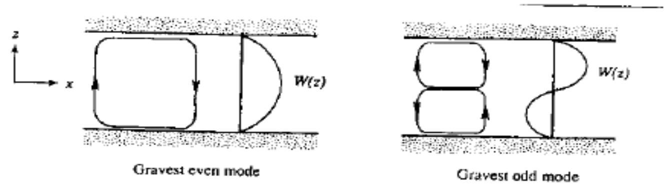

Fig. 11.3 Flow pattern and eigenfunction structure of the gravest even mode and the gravest odd mode in the Bénard problem.

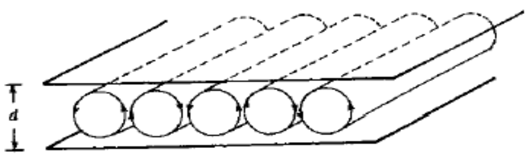

Fig. 11.5 Convection rolls in a Bénard problem.

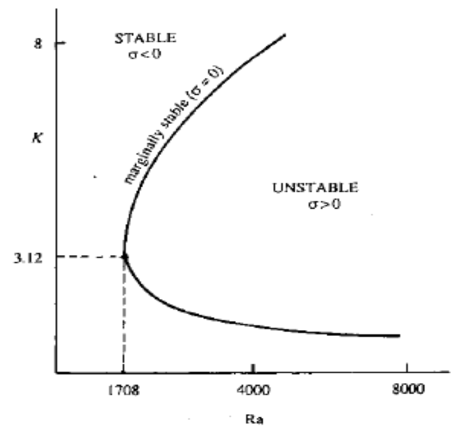

Fig. 11.4 Stable and unstable regions for Bénard convection.

(b) finger/oscillatory instability: hot/salty over cold/fresh water and vise versa.

$(Rs - Ra)_{cr} = 657$

$$Rs = g\beta d^4 \left(ds/dz\right)/\nu k_s$$

$$\rho = \rho_0(1 - \alpha\Delta T + \beta\Delta S)$$

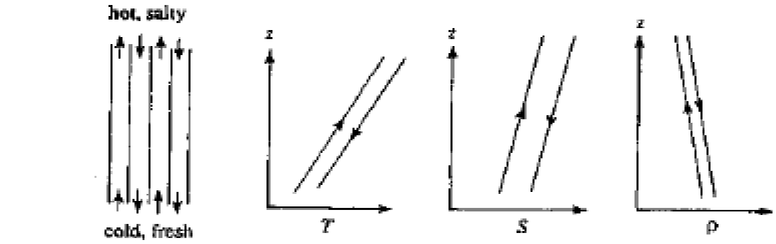

(a) Finger regime

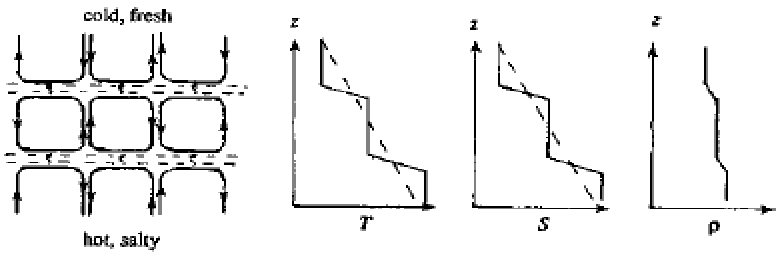

(b) Diffusive regime

Fig. 11.7 **Two kinds of double-diffusive instabilities. (a) Finger instability, showing up- and down-going salt fingers and their temperature, salinity, and density. Arrows indicate direction of motion.** (b) Oscillating instability, finally resulting in a series of convecting layers separated by "diffusive" interfaces. Across these interfaces T and S vary sharply, but heat is transported much faster than salt.

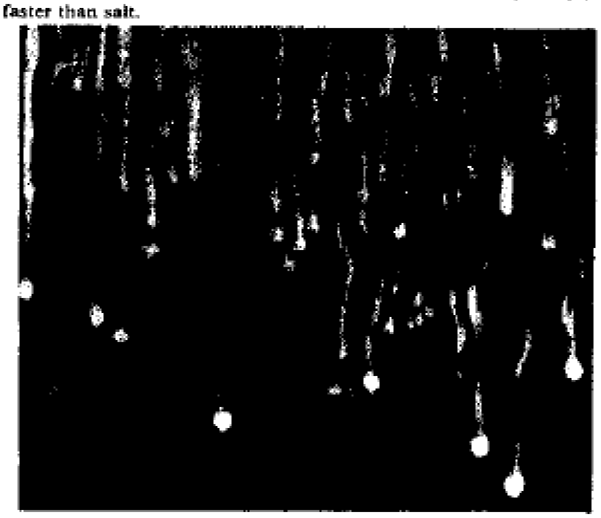

Fig. 11.8 Salt fingers, produced by pouring salt solution on top of a stable temperature gradient. Flow visualization by fluorescent dye and a horizontal beam of light. [From Turner (1985).]

(c) Centrifugal instability: Taylor Problem

Bernard Instability: buoyant force > viscous force
Taylor Instability: Couette flow between two rotating cylinders where centrifugal force (outward

from center opposed to centripetal force) > viscous force.

$$Ta = \frac{r_i c\left(\Omega_i^2 - \Omega_o^2\right)}{\nu^2} \qquad c = r_0 - r_i \ll r_i$$

$$= centrifugal\ \ force / viscous\ force$$

$$Ta_{cr} = 1708 \qquad \alpha_{cr}c = 3.12 \quad \rightarrow \quad \lambda_{cr} = 2c$$

$$Ta_{trans} = 160{,}000$$

Square counter rotating vortex pairs with helix streamlines

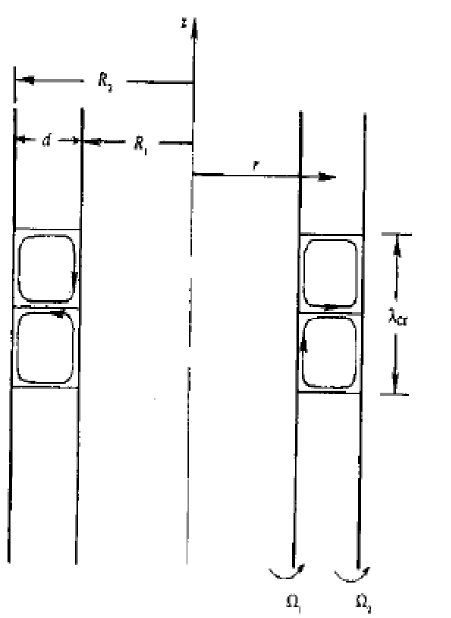

Fig. 11.10 Definition sketch of instability in rotating Couette flow.

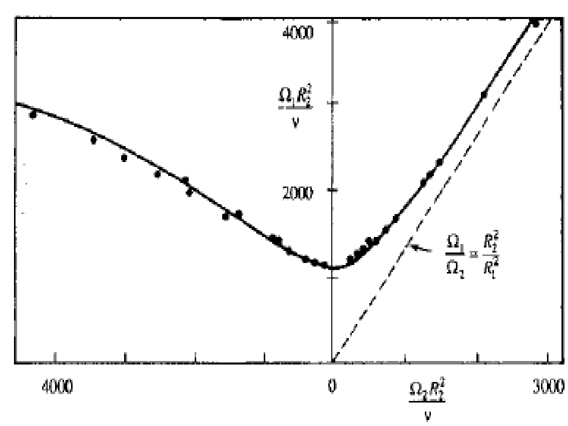

Fig. 11.11 G. I. Taylor's observation and narrow-gap calculation of marginal stability in rotating Couette flow of water. The ratio of radii is $R_2/R_1 = 1.14$. The region above the curve is unstable. The dashed line represents Rayleigh's inviscid criterion, with the region to the left of the line representing instability.

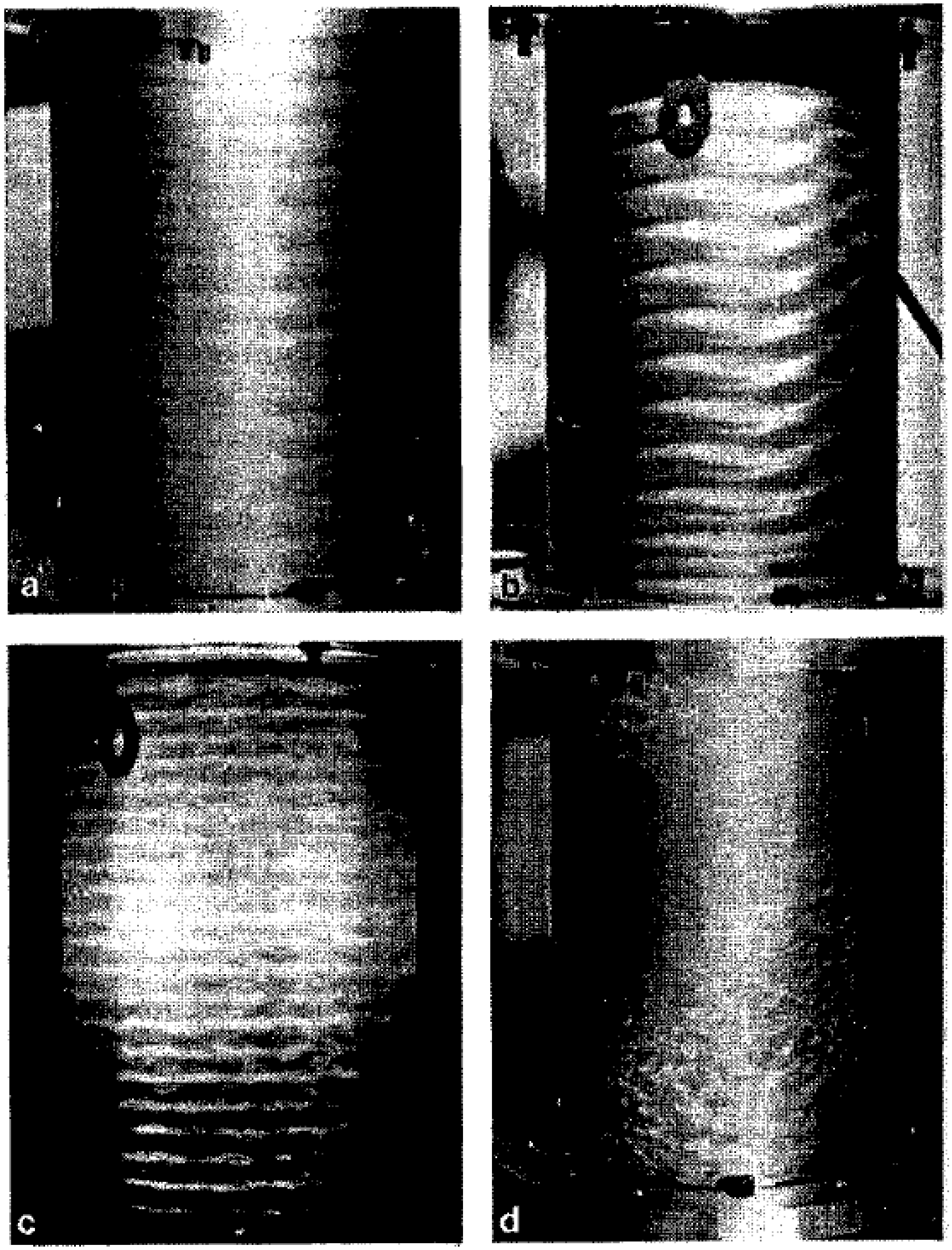

Fig. 11.12 Instability of rotating Couette flow. Panels a, b, c, and d correspond to increasing Taylor number. [From Coles (1965).]

(d) Gortler Vortices

Longitudinal vortices in concave curved wall boundary layer induced by centrifugal force and related to swirling flow in curved pipe or channel induced by radial pressure gradient and discussed later with regard to minor losses.

For $\delta/R > .02\sim.1$ and $Re_\delta = U\delta/\upsilon > 5$

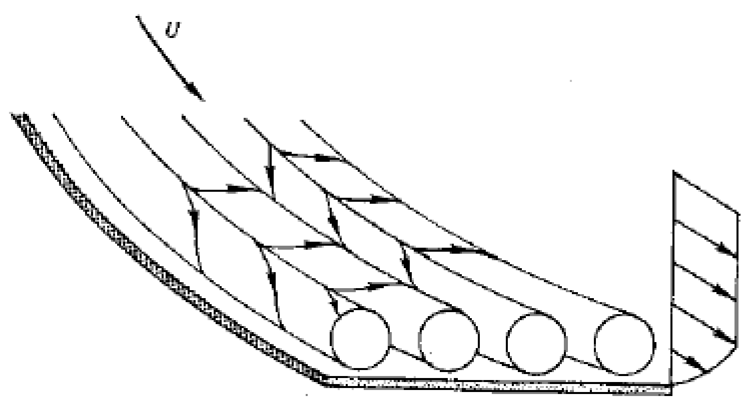

Fig. 11.13 Görtler vortices in a boundary layer along a concave wall.

(e) Kelvin-Helmholtz instability

Instability at interface between two horizontal parallel streams of different density and velocity with heavier fluid on bottom, or more generally ρ=constant and U = continuous (i.e. shear layer instability e.g. as per flow separation). Former case, viscous force overcomes stabilizing density stratification.

$$g\left(\rho_2^2-\rho_1^2\right)<\alpha\rho_1\rho_2\left(U_1-U_2\right)^2 \quad \rightarrow \quad c_i>0 \text{ (unstable)}$$

$U_1 \neq U_2$ *large* α *i.e. short* λ always unstable

Vortex Sheet

$\rho_1=\rho_2 \quad \rightarrow \quad c_i=\frac{1}{2}(U_1+U_2) \qquad > 0$

Therefore always unstable

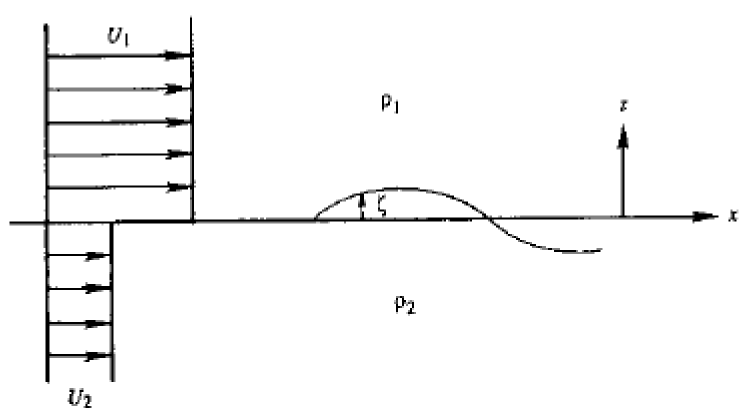

Fig. 11.14 Discontinuous shear across a density interface.

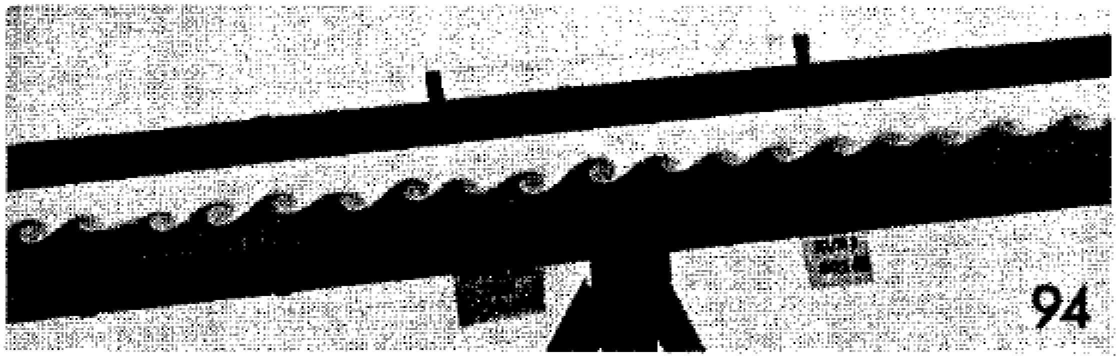

Fig. 11.16 Kelvin–Helmholtz instability generated by tilting a horizontal channel containing two liquids of different densities. The lower layer is dyed. Mean flow in the lower layer is down the plane and that in the upper layer is up the plane. [From Thorpe (1971).]

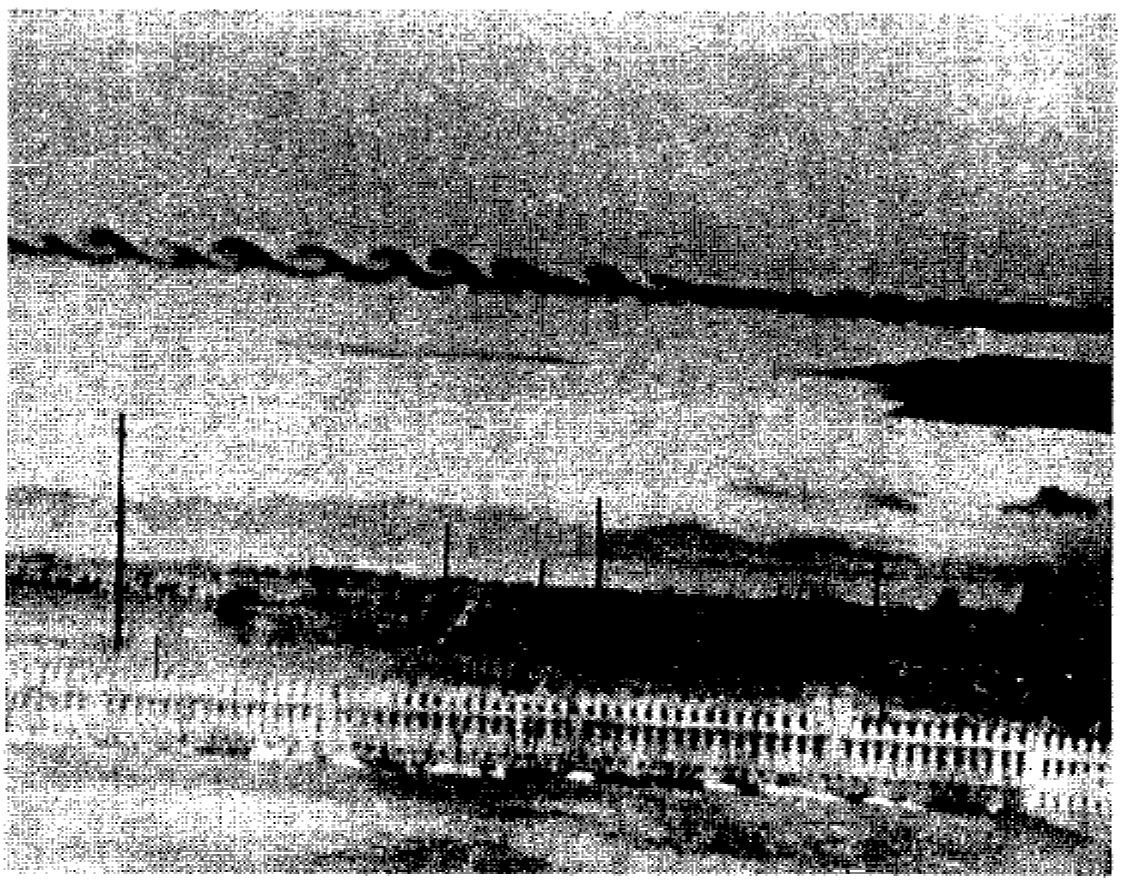

Fig. 11.17 Billow cloud near Denver, Colorado. [From Drazin and Reid (1981).]

(2) Transition from laminar to turbulent flow

Not all laminar flows have different equilibrium states, but all laminar flows for sufficiently large Re become unstable and undergo transition to turbulence.

Transition: change over space and time and Re range of laminar flow into a turbulent flow.

$$\mathrm{Re}_{cr} = \frac{U\delta}{\upsilon} \sim 1000 \qquad \delta = \textit{transverse viscous thickness}$$

$\mathrm{Re}_{trans} > \mathrm{Re}_{cr}$ with $x_{trans} \sim 10\text{-}20\ x_{cr}$

Small-disturbance (linear) stability theory can predict Re_{cr} with some success for parallel viscous flow such as plane Couette flow, plane or pipe Poiseuille flow, boundary layers without or with pressure gradient, and free shear flows (jets, wakes, and mixing layers).

Note: No theory for transition, but recent DNS helpful.

Outline linearized stability theory for parallel viscous flows: select basic solution of interest; add disturbance; derive disturbance equation; linearize and simplify; solve for eigenvalues; interpret stability conditions and draw thumb curves.

$$u = \bar{u} + \hat{u}$$
$$v = \bar{v} + \hat{v}$$
$$p = \bar{p} + \hat{p}$$

$\bar{u}, \bar{v} =$ mean flow, which is solution steady NS

$\hat{u}, \hat{v} =$ small 2D oscillating in time disturbance is solution unsteady NS

$$\hat{u}_t + \bar{u}\hat{u}_x + \hat{u}\bar{u}_x + \bar{v}\hat{u}_y + \hat{v}\bar{u}_y = -\frac{1}{\rho}\hat{p}_x + \upsilon\nabla^2\hat{u}$$
$$\hat{v}_t + \bar{u}\hat{v}_x + \hat{u}\bar{v}_x + \bar{v}\hat{v}_y + \hat{v}\bar{v}_y = -\frac{1}{\rho}\hat{p}_x + \upsilon\nabla^2\hat{u}$$
$$\hat{u}_x + \hat{v}_x = 0$$

Linear PDE for $\hat{u}$, $\hat{v}$, $\hat{p}$ for ($\bar{u}$, $\bar{v}$, $\bar{p}$) known.

Assume disturbance is sinusoidal waves propagating in x direction at speed c: Tollmien-Schlicting waves.

$$\hat{\Psi}(x, y, t) = \phi(y)e^{i\alpha(x-ct)}$$
$$\hat{u} = \frac{\partial\hat{\psi}}{\partial y} = \phi' e^{i\alpha(x-ct)}$$
$$\hat{v} = -\frac{\partial\hat{\Psi}}{\partial x} = -i\alpha\phi e^{i\alpha(x-ct)}$$

Stream function
y =distance across shear layer

$\hat{u}_x + \hat{v}_y = 0$ Identically!

$\alpha = \alpha_r + i\alpha_i$ = *wave number* = $2\pi/\lambda$

$c = c_r + ic_i$ = *wave speed* = ω/α

Where λ = *wave length and* ω =*wave frequency*

Temporal stability:

Disturbance ($\alpha = \alpha_r$ only and c_r real)

c_i	> 0	unstable
	$= 0$	neutral
	< 0	stable

Spatial stability:

Disturbance ($c\alpha$ = real only)

α_i	< 0	unstable
	$= 0$	neutral
	> 0	stable

Inserting $\hat{u}$, $\hat{v}$ into small disturbance equations and eliminating $\hat{p}$ results in Orr-Sommerfeld equation:

$$\overbrace{(u-c)(\phi''-\alpha^2\phi)-u''\phi}^{inviscid\ \ Raleigh\ equation} = -\frac{i}{\alpha\,\mathrm{Re}}(\phi^{IV}-2\alpha^2\phi''+\alpha^4\phi)$$

$$u=\bar{u}/U \qquad Re=UL/\upsilon \qquad y=y/L$$

4th order linear homogeneous equation with homogenous boundary conditions (not discussed here) i.e. eigen-value problem, which can be solved albeit not easily for specified geometry and ($\bar{u}$, $\bar{v}$, $\bar{p}$) solution to steady NS.

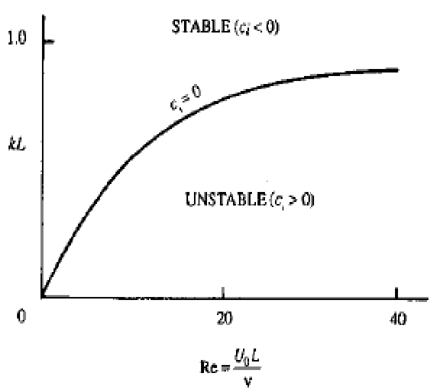

Fig. 11.23 Marginal stability curve for a shear layer $u = U_0 \tanh(y/L)$.

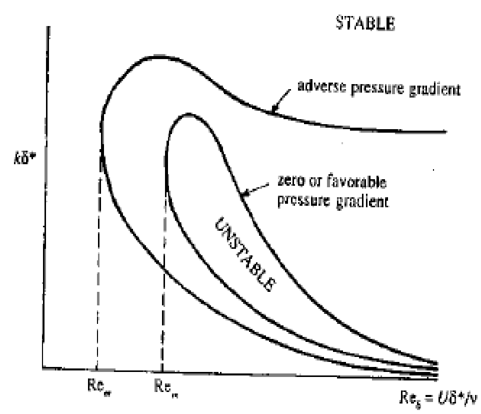

Fig. 11.24 Sketch of marginal stability curves for a boundary layer with favorable and adverse pressure gradients.

TABLE 11.1 Linear Stability Results of Common Viscous Parallel Flows

Flow	$U(y)/U_0$	Re_{cr}	Remarks
Jet	$\mathrm{sech}^2(y/L)$	4	
Shear layer	$\tanh(y/L)$	0	Always unstable
Blasius		520	Re based on δ^*
Plane Poiseuille	$1-(y/L)^2$	5780	L = half width
Pipe flow	$1-(r/R)^2$	∞	Always stable
Plane Couette	y/L	∞	Always stable

Although difficult, methods are now available for the solution of the O-S equation. Typical results as follows

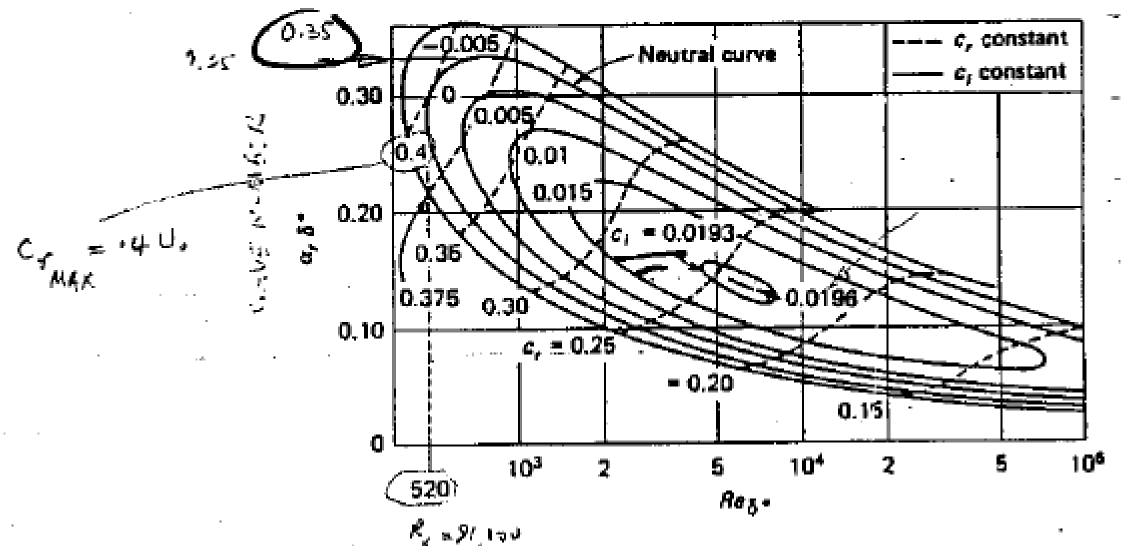

FIGURE 5-6
Amplification curves for the Blasius flat-plate boundary layer. [*After Wazzan, Okamura, and Smith (1968a).*]

(1) Flat Plate BL:

$$Re_{crit} = \frac{U\delta^{+}}{\upsilon} = 520$$

(2) $\alpha\delta^* = 0.35$

$\rightarrow$ $\lambda_{min} = 18\ \delta^* = 6\ \delta$ (*smallest unstable* λ)

$\therefore$ unstable T-S waves are quite large

(3) c_i = constant represent constant rates of damping ($c_i < 0$) or amplification ($c_i > 0$). $c_{i\,max} = .0196$ is small compared with inviscid rates indicating a gradual evolution of transition.

(4) $(c_r/U_0)_{max} = 0.4 \rightarrow$ unstable wave travel at average velocity.

(5) $Re_{\delta^* crit} = 520 \rightarrow Re_{x\ crit} \sim 91{,}000$

Exp: $Re_{x\ crit} \sim 2.8 \times 10^6$ ($Re_{\delta^* crit} = 2{,}400$) if care taken, i.e., low free stream turbulence

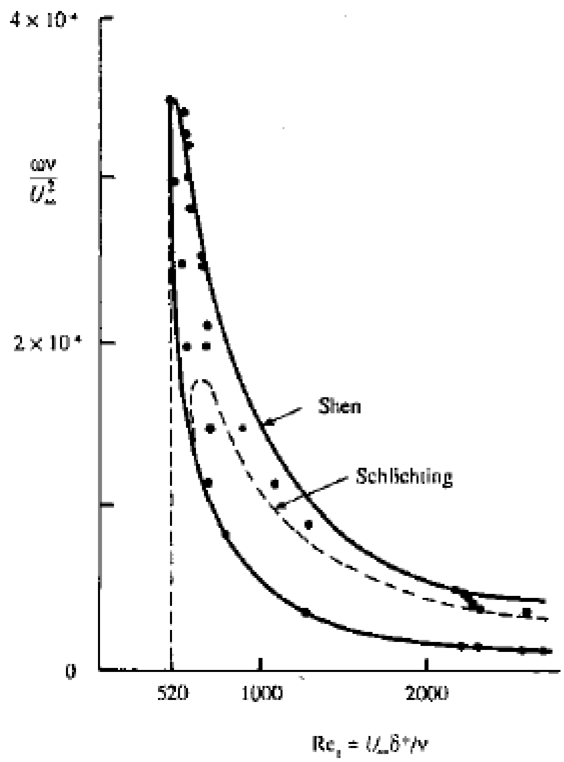

Fig. 11.26 Marginal stability curve for a Blasius boundary layer. Theoretical solutions of Shen and Schlichting are compared with experimental data of Schubauer and Skramstadt.

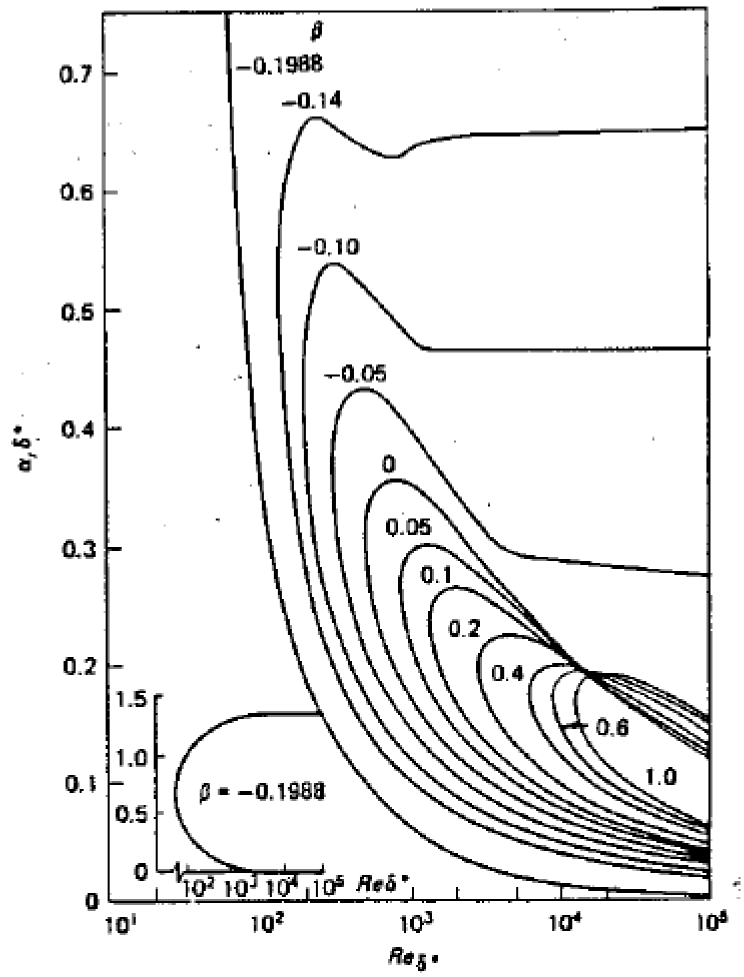

FIGURE 5-7
Neutral-stability curves for the Falkner-Skan boundary-layer profiles. (*After*

Falkner-Skan Profiles:

(1) strong influence of β

$Re_{crit} \uparrow$ $\beta > 0$ $\uparrow$ fpg

$Re_{crit} \downarrow$ $\beta < 0$ $\downarrow$ apg

$Re_{\delta^* crit}$:
67 sep bl
520 fp bl
12,490 stag point bl

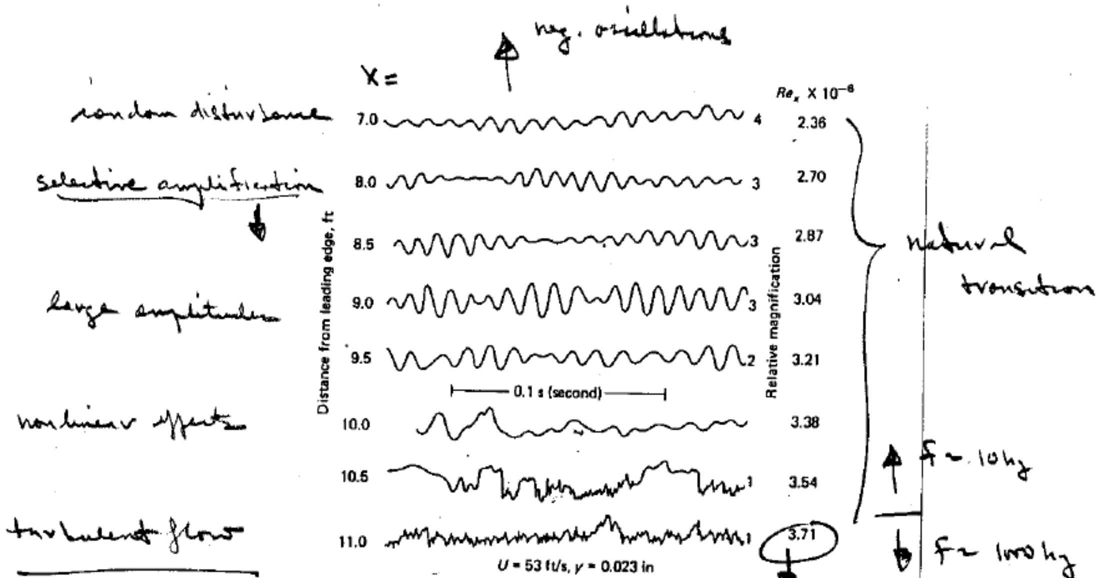

FIGURE 5-8
Hot-wire oscillograms showing natural transition from laminar to turbulent flow on a flat plate. [*After Schubauer and Skramstad (1947).*]

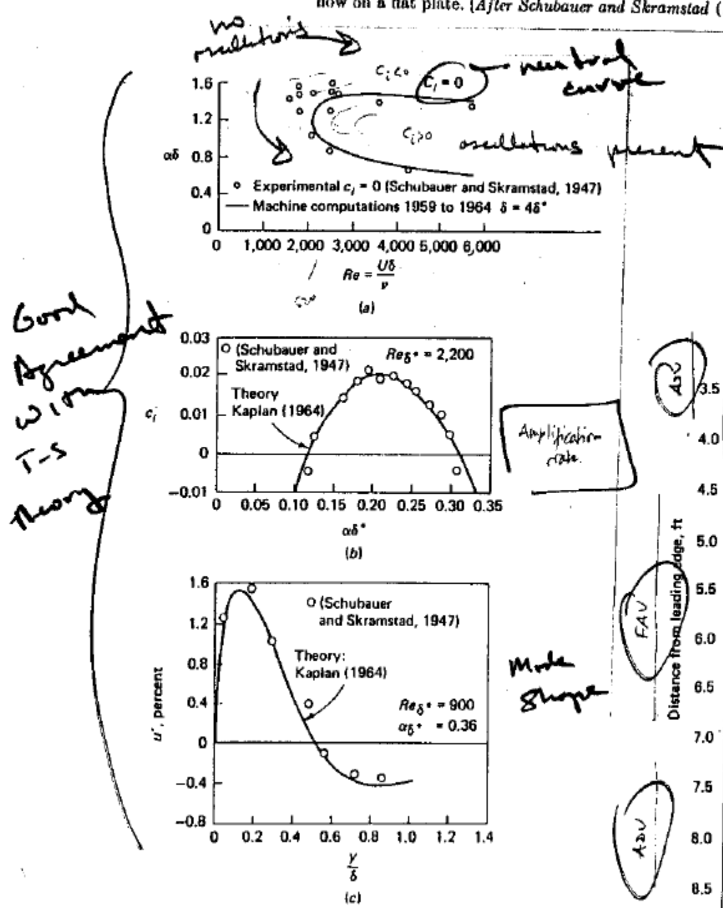

IGURE 5-9
omparison of stability theory for the Blasius profile with the flat-plate experiment of Schubauer and Skramstad (1947): (*a*) neutral curve; (*b*) amplification actors; (*c*) longitudinal velocity fluctuation.

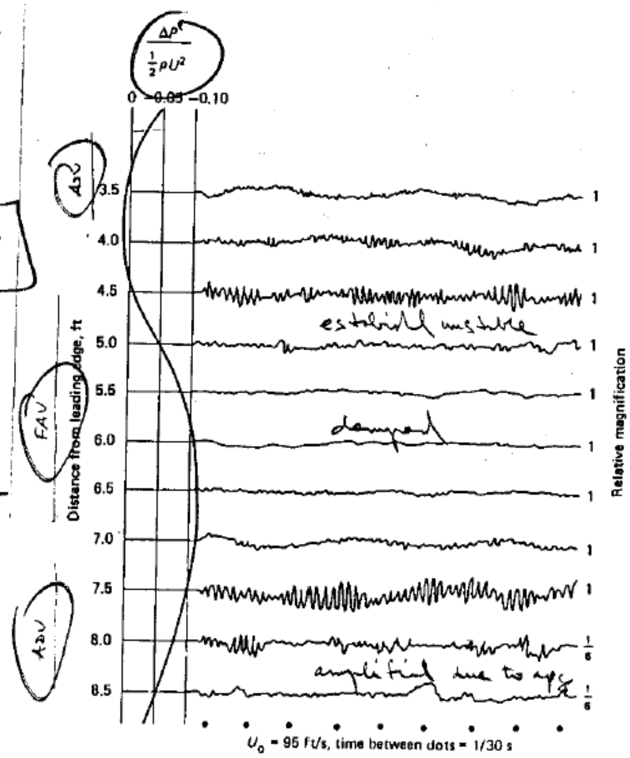

FIGURE 5-10
Effect of pressure gradient on laminar-boundary-layer oscillations. [*After Schubauer and Skramstad (1947).*]

αL

.007

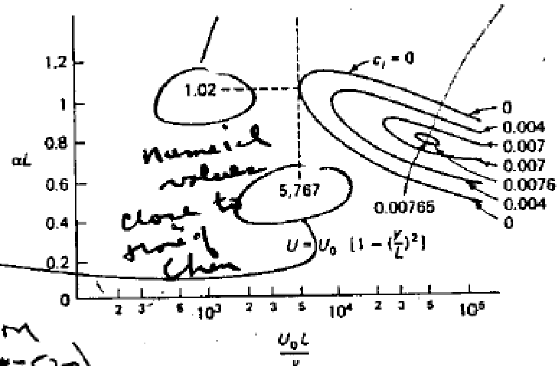

~5% accuracy

Numerical values close to those of Chen

large compared with Blasius (based on $Re_{\delta^*_{cr}} = 520$)

asymptotic method

FIGURE 5-11
Stability diagram for plane Poiseuille flow. [*After Shen* (1954).]

Couette Flow with p_x : $U = U_0(1 - y^2/L^2)$

70,000

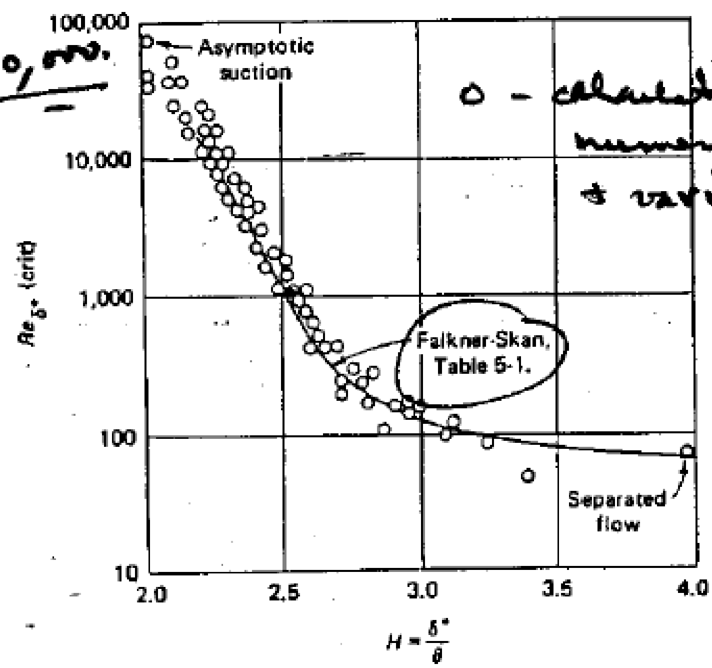

o - calculations from numerous sources & variety of flows

70

FIGURE 5-12
Correlation of the critical Reynolds number with the profile shape factor for laminar flow.

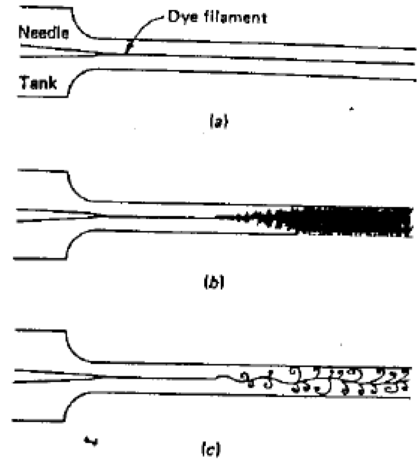

FIGURE 5-24
The classic pipe-flow dye experiment of Reynolds (1883): (*a*) low speed: laminar flow; (*b*) high speed: turbulent flow; (*c*) spark photograph of condition (*b*).

Our overall picture of the transition process in quiet flow past a smooth flat plate consists of the following processes as one moves downstream:

development of regions of high localized shear

1. Stable laminar flow near the leading edge
2. Unstable two-dimensional Tollmien-Schlichting waves
3. Development of three-dimensional unstable waves and hairpin eddies
4. Vortex breakdown at regions of high localized shear
5. Cascading vortex breakdown into fully three-dimensional fluctuations
6. Formation of turbulent spots at locally intense fluctuations
7. Coalescence of spots into fully turbulent flow

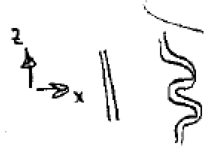

Extent and details of these processes depends on Re and many other factors (geometry, pg, free-stream, turbulence, roughness, etc).

Rapid development of span-wise flow, and initiation of nonlinear processes

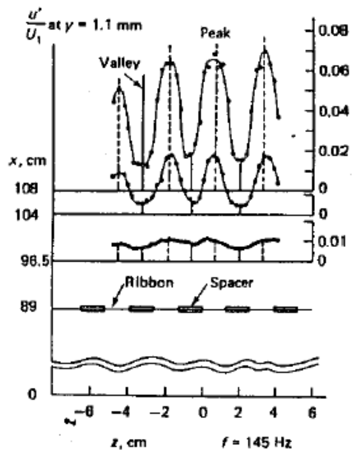

FIGURE 5-25
Development of spanwise variations in the streamwise velocity fluctuation downstream of a vibrating ribbon with spacers. [*After Klebanoff, Tidstrom, and Sargent (1962).*]

- stretched vortices disintigrate
- cascading breakdown into families of smaller and smaller vortices
- onset of turbulence

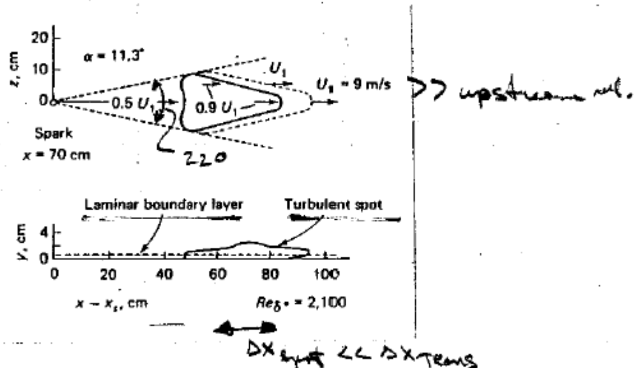

FIGURE 5-26
Plan and elevation of the measured growth of a turbulent spot. [*After Schubauer and Klebanoff (1955).*]

Note: apg may undergo much more abrupt transition. However, in general, pg effects less on transition than on stability

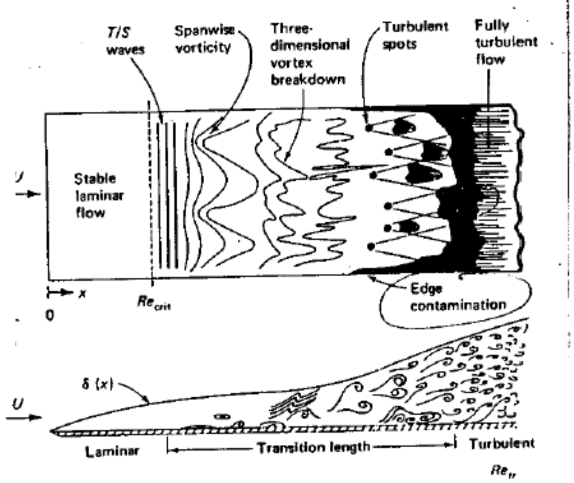

FIGURE 5-27
Idealized sketch of transition process on a flat plate.

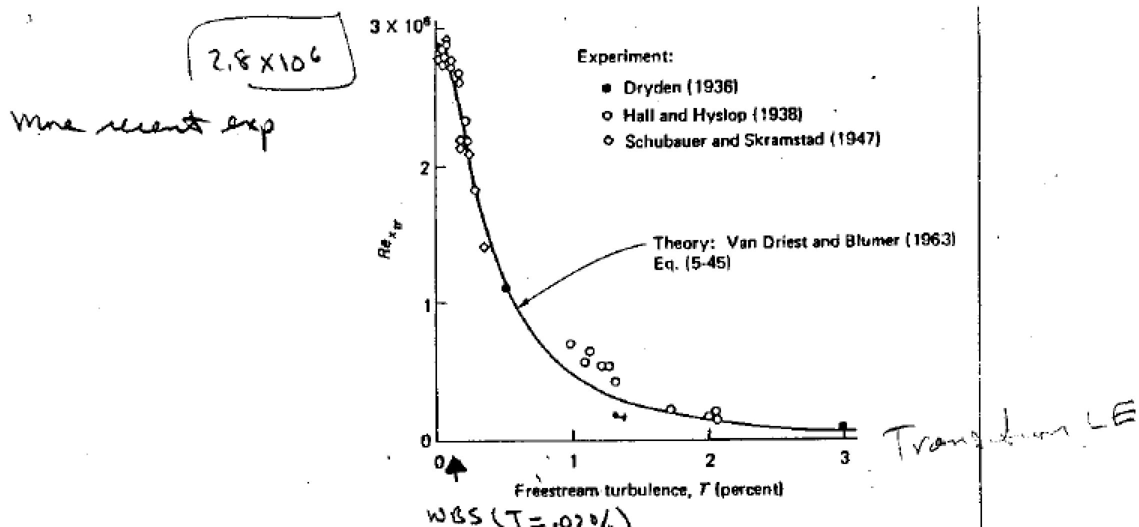

FIGURE 5-28
Comparison of theory and experiment for transition Reynolds number on a flat plate at various levels of freestream turbulence. [*After van Driest and Blumer (1963)*.]

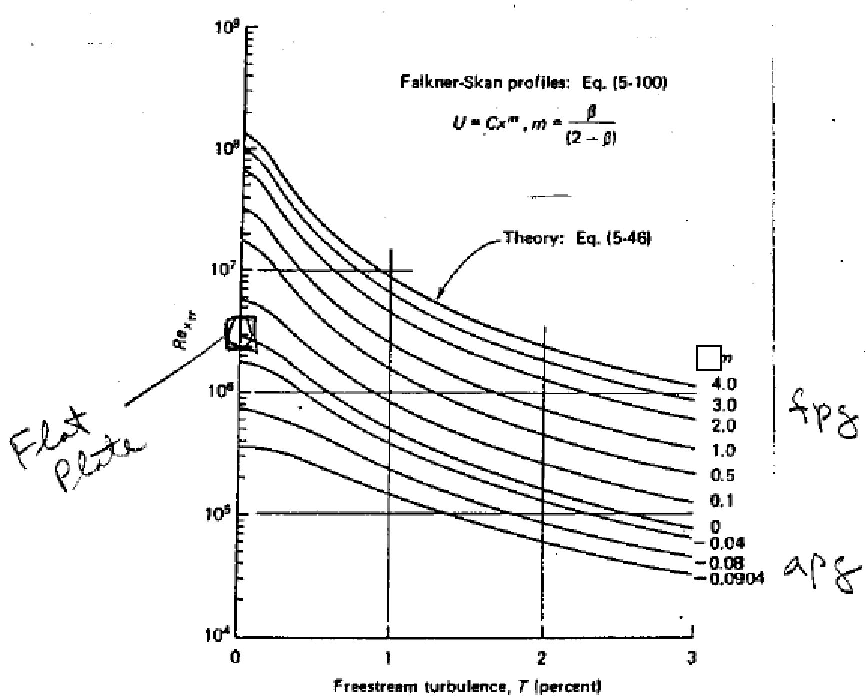

FIGURE 5-29
Effect of pressure gradient and freestream turbulence on transition Reynolds number. [*After van Driest and Blumer (1963)*.]

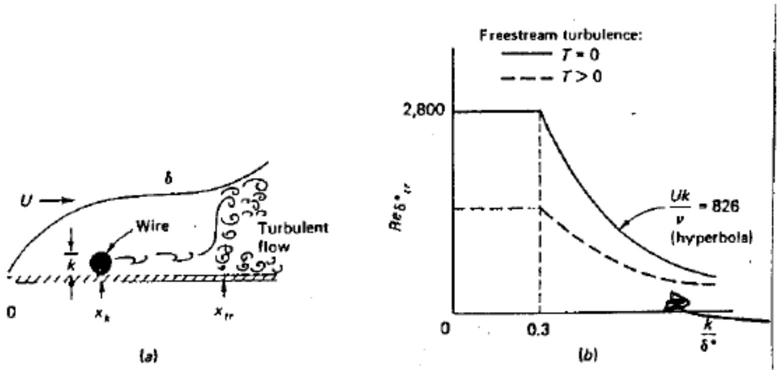

effect of T

FIGURE 5-30
Idealized effect of two-dimensional roughness on transition: (a) flat plate with trip wire; (b) transition data.

effect of T removed if data normalized to same smooth wall amplitude

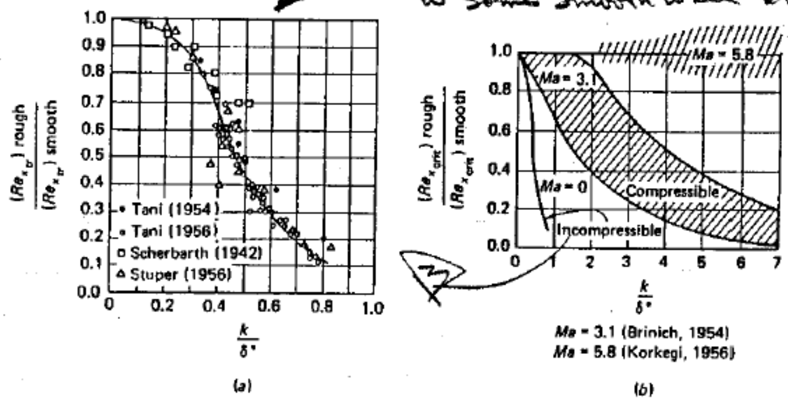

FIGURE 5-31
Flat-plate, two-dimensional roughness transition data normalized to eliminate freestream turbulence effects: (a) incompressible flow [*After Dryden (1953)*]; (b) compressible flow.

Some recent work concerns recovery distance: